Published in final edited form as:
Surgery. 2009 March ; 145(3): 294–302. doi:10.1016/j.surg.2008.11.004.

Diurnal expression of the rat intestinal sodium-glucose co-transporter SGLT1 is independent of local luminal factors

Adam T. Stearns[1,2,3], **Anita Balakrishnan**[1,2,4], **David B. Rhoads**[2,5], **Stanley W. Ashley**[1,2], and **Ali Tavakkolizadeh**[1,2,*]

[1] Department of Surgery, Brigham & Women's Hospital, 75 Francis Street, Boston, Massachusetts 02115. United States of America

[2] Harvard Medical School, Boston, Massachusetts 02115. United States of America

[3] Department of Physiology, Anatomy & Genetics, University of Oxford, South Parks Road, Oxford. OX1 3QX. United Kingdom

[4] School of Clinical Sciences, Division of Gastroenterology, University of Liverpool, Crown Street, Liverpool. L69 3GE. United Kingdom

[5] Pediatric Endocrine Unit, MassGeneral Hospital *for* Children, 55 Fruit Street, Boston, Massachusetts 02114. United States of America

Abstract

Introduction—The intestinal sodium-glucose cotransporter SGLT1 is responsible for all secondary active transport of dietary glucose, and thus presents a potential therapeutic target for obesity and diabetes. SGLT1 expression varies with a profound diurnal rhythm, matching expression to nutrient intake. The mechanisms entraining this rhythm remain unknown. We investigated the role of local nutrient signals in diurnal SGLT1 entrainment.

Methods—Male Sprague-Dawley rats, acclimatized to a 12: 12 light: dark cycle, underwent laparotomy with formation of isolated proximal jejunal loops (Thiry-Vella loops). Animals were recovered for 10 days before harvesting at four six-hourly intervals (Zeitgeber times ZT3, ZT9, ZT15, ZT21 where ZT0 is lights-on; n=6–8). SGLT1 expression was assessed in protein and mRNA extracts of mucosa harvested from both isolated loops (LOOP) and remnant jejunum (JEJ).

Results—Isolated loops were healthy but atrophic, with minimal changes to villus architecture. A normal anticipatory rhythm was observed in *Sglt1* transcription in both LOOP and JEJ, with peak signal at ZT9 (2.7-fold, $p<0.001$). Normal diurnal rhythms were also observed in protein signal, with peak expression in both LOOP and JEJ at ZT9 to 15 (2.1-fold, $p<0.05$). However, an additional more mobile polypeptide band was also observed in all LOOP samples, but not in JEJ samples (61kDa versus 69kDa). Enzymatic deglycosylation suggested this to be deglycosylated SGLT1.

Conclusions—Persistence of SGLT1 rhythmicity in isolated loops indicates that diurnal induction is independent of local luminal nutrient delivery, and suggests reliance on systemic entrainment

*Corresponding author: email: atavakkoli@partners.org, Phone: 617-732-6337, Fax: 617-734-0336.

This manuscript was presented in part at the 3rd Annual Academic Surgical Congress, Huntington Beach, California, February 2008.

Conflicts of Interest
No authors have any conflicts of interest to declare.

pathways. However, local luminal signals may regulate glycosylation and therefore post-translational handling of SGLT1.

Keywords

Thiry-vella loop; glucose transport; diurnal rhythm; circadian

Introduction

The intestinal sodium-glucose cotransporter SGLT1 is the archetypal sodium-dependent symporter, and is responsible for all intestinal secondary active transport of glucose[1]. SGLT1 is located on the brush-border membrane of enterocytes throughout the small bowel, and co-transports glucose into the enterocyte along an electrochemical sodium gradient. Glucose then exits the enterocyte through basolateral GLUT2 facilitated glucose transporters into the portal system[2]. Transporter-mediated uptake of glucose accounts for the majority of intestinal glucose uptake under physiological conditions[3, 4], and studies show the competitive inhibitor phloridzin effectively abolishes glucose uptake[4, 5]. As such, SGLT1 represents a putative therapeutic target for obesity and associated type 2 diabetes mellitus, highlighted by emerging evidence for dysregulation of SGLT1 in these disease states[6–10]. Despite the importance of SGLT1, both in normal intestinal physiology and in disease, its regulation is not completely understood- limiting development of potential treatment strategies.

The human SGLT1 protein has 664 amino acids with a single *N*-glycosylation site at Asn248 (approximately 9–11kDa)[11–13]. The holoprotein runs on SDS-PAGE with an apparent molecular weight of 68–74kDa[2,13,14]. Glycosylation does not appear necessary for SGLT1 function, but occurs as the protein trafficks the endoplasmic reticulum and *trans*-Golgi apparatus[13,15,16].

We and others have shown that intestinal SGLT1 expression is tightly matched to expected and actual nutrient delivery[17–19]. Most mammals preferentially feed with a diurnal periodicity, and glucose transport has repeatedly been shown to vary with a diurnal rhythm to match transport capacity with expected nutrient intake[5,20–22]. At a molecular level, SGLT1 protein abundance varies over a 2 to 3-fold range, with peak expression shortly after nutrient intake begins. In nocturnally feeding rats, this is soon after the onset of darkness. The increase in protein is preceded by several hours by an increase in *Sglt1* mRNA abundance, which varies over a 5-fold range. This diurnal rhythmicity has been confirmed in primates (Rhesus monkeys), although off-set by 12 hours reflecting the day-time feeding preferences of these animals[17].

The cuing mechanisms involved in the establishment of diurnal rhythms in SGLT1 remain unknown. Diurnal SGLT1 rhythms in rats are greatly affected by preceding feeding schedules, and persist during brief fasting for several days[19]. Imposing a daylight feeding rhythm on nocturnal rodents leads to a rapid shift in the phase of both transcriptional and SGLT1 protein rhythms, to match the imposed nutrient intake patterns[19]. Diurnal rhythms in glucose transport capacity are ablated by continuous total parenteral nutrition, but maintained by pulsed total parenteral nutrition[23], suggesting that alternating nutrient delivery is the cuing factor.

To investigate how nutrients may entrain SGLT1, we examined SGLT1 rhythmicity in isolated Thiry-Vella loops. We now describe persistence of diurnal rhythms in isolated loops, as well as suggesting luminal contents may regulate the post-translational handling of SGLT1.

Methods

Animals

All studies were prospectively approved by the Harvard Medical Area Standing Committee on Animals. Male Sprague Dawley rats (350–361g, Harlan, Indianapolis, IN) were purchased and acclimatized to a 12:12 hour light-dark cycle under constant humidity and temperature for seven days. Lights were switched on at 7AM. Rat chow and water was provided *ad libitum* throughout the experiment. On the day of operation, animals were anesthetized with sodium pentobarbital (50mg/kg IP injection, Ovation Pharmaceuticals, Deerfield, IL) and underwent formation of a Thiry-Vella isolated jejunal loop. The animal was placed on a warming pad, and under aseptic conditions a midline laparotomy was performed, and the jejunum transected at 5cm and 22cm distal to the ligament of Trietz. The intervening 17cm length of jejunum (the Thiry-Vella loop) was exteriorized on its mesenteric pedicle to the right of the midline. Two small incisions were made in the abdominal wall, and the proximal and distal cut ends of bowel were exteriorized before fashioning ostomies using interrupted 6/0 PDS. A tacking suture was also placed between the antimesenteric aspect of the bowel, just within the abdominal cavity, and the peritoneum to prevent stomal prolapse. The proximal and distal cut ends of the remaining jejunum were anastomosed to restore enteric continuity. Stay sutures, again interrupted 6/0 PDS, were placed in the mesenteric and antimesenteric aspects, in particular ensuring good apposition at the mesenteric corner. The anastomosis was then completed using a total of 10–12 interrupted sutures. At all times, the bowel was kept damp using sterile swabs soaked with normal saline. A thorough lavage was then performed (3× 20mL warmed normal saline) before closing the abdominal wall in two layers using a 3-0 vicryl suture. Post-operatively, animals were recovered in a warm box before return to the animal facility. Buprenorphine (0.05mg/kg sc BD; Bedford Laboratories, Bedford, OH) was provided as analgesia for 48 hours. A single dose of ketoprofen 5.0 mg/kg sc (Fort Dodge Animal Health, Fort Dodge, IA) was also administered post-operatively.

Animals were maintained for 10 days post-operatively, with *ad libitum* access to rat chow and tap water. This survival duration was chosen as preliminary studies showed this to be a week after weight gain recommenced. Thiry-Vella loops were flushed daily for the first three days post-operatively using 5–10mL of normal saline, to remove any luminal debris. At the end of the study, 6–8 rats were harvested at each of four times: Zeitgeber time ZT3, ZT9, ZT15 and ZT21 (ZT0 is defined as lights on; harvest times correspond to 10AM, 4PM, 10PM, 4AM, respectively). Rats were anesthetized using sodium pentobarbital 50mg/kg IP before laparotomy. Any adhesions were gently taken down and the loop and jejunum mobilized. The intact jejunum was flushed with excess ice-cold phosphate-buffered saline, pH7.4, while on its mesenteric pedicle. 14cm of jejunum was then excised from 1cm distal to the anastomosis, opened on a glass plate over ice, before scraping with glass microscope slides to retrieve mucosa. Jejunal mucosa (JEJ) was then divided into four aliquots and flash frozen in liquid nitrogen. The process was repeated for Thiry-Vella loops (LOOP), harvesting mucosa from the bowel less 1cm from either stoma.

Morphology

At harvest, 1cm sections of each of LOOP and JEJ were harvested at ZT15 (10PM, peak glucose uptake in previous experiments) were placed in 10% buffered formalin and allowed to equilibrate for at least 24 hours at 4°C. Sections were then dehydrated in ethyl alcohol and embedded in paraffin, ensuring the section of bowel was orientated transversely to the plane of sectioning.

Sections were then cut at 4μm thickness on a microtome, mounted on Superfrost slides and deparaffinized in 100% xylene. After rehydration, slides were stained with hematoxylin and

eosin before coverslipping. Slides were examined under a light microscope (Olympus BX50, Olympus, Center Valley, PA) at 40–400x magnification, and the following parameters measured in triplicate for each animal: maximum diameter of the intestine (major axis of the ellipse); diameter along the minor axis (perpendicular to major axis at the mid-point); the villus height; villus width at tip and base; crypt depth; and enterocyte diameter at mid-villus (as measured by number of nuclei observed over 125μm). Representative samples were photographed under 40x magnification (Nikon Labophot, Melville, NY; Polaroid DMC2 camera and software, Polaroid, Concord, MA), and the photomicrographs for each section joined as a composite using Adobe Photoshop CS2 (Adobe, San Jose, CA).

mRNA Analysis

Total cellular RNA was extracted from mucosa using the mirVANA mRNA extraction kit (Ambion, Austin, TX). Mucosa was homogenized in ice-cold lysis buffer using a pipette, and RNA extracted into phenol: chloroform. Nucleic acids were precipitated using absolute alcohol, and adsorbed to a ceramic filter. After appropriate washes, mRNA was eluted and quantified using a spectrophotometer (Spectramax M5; Molecular Devices, Sunnyvale, CA). mRNA was then reverse transcribed using a Superscript III kit (Invitrogen, Carlsbad, CA) with oligo(DT) priming, according to protocols provided by the manufacturer. All reverse transcription, and subsequent quantitative PCR was performed simultaneously, to minimize variability. After appropriate dilution of the cDNA library, qPCR was performed using SYBR green master mix (Applied Biosystems, Foster City, CA) and primers against rat *Sglt1* and *Actin*. Primers used were as follows: *Sglt1* 5′-CCAAGCCCATCCCAGACGTACACC and 5′-CTTCCTTAGTCATCTTCGGTCCTT; *Actin* 5′-GGATCAGCAAGCAGGAGTACGA and 5′-AACGCAGCTCAGTAACAGTCCG. qPCR was performed on 384-well plates using an ABI7900HT thermal cycler (Applied Biosystems), with 2 min at 50 C then 10 min 95°C, followed by 40 cycles of 15 sec 95°C and 1 min 60°C. A dissociation protocol was also employed, enabling verification of a single amplicon. Use of 384-well plates allowed simultaneous analysis for *Sglt1* and for *Actin*, again minimizing variation within the process. *Sglt1* expression was normalized against *Actin* signal as a loading control.

Whole cell protein extraction and Western Immunoblotting

An aliquot of mucosa was thawed in 1ml chilled Triton X lysis buffer (Boston Bioproducts, Ashland, MA) containing 10μL protease inhibitor (Sigma, St Louis, MO). On ice, the sample was homogenized for 30 seconds with a polytron, before sonication for 60 seconds. Whole cell protein was separated on a refrigerated microcentrifuge at 11000g for 15 minutes. Protein was quantified using the bicinchoninic acid assay, against bovine serum albumen standards, and stored at −80°C prior to further analysis. Protein samples were thawed on ice, and 50–60μg total cell lysate protein dissolved in LDS buffer before linearizing at 95°C for 6 minutes. After cooling, samples were loaded to 10% bis-tris gels and run at 100V in MOPS running buffer (Invitrogen) to maximize band separation in the 40–80kDa molecular weight range. On each gel, a representative sample from an animal from each time point was included. Both LOOP and JEJ samples were included in each gel, as was a standard sample used to compare gels. Gels were then transferred to PVDF membranes (Invitrogen), before blocking the membrane with 10% casein (Vector Laboratories, Burlingame, CA) and incubating for two hours with anti-SGLT1 antibody (1:4000, Chemicon International, Temecula, CA) in PBS-tween containing 5% casein. After further washing, the membranes were probed with peroxidase labeled anti-rabbit antibodies (1:5000, Vector Laboratories), then washed again. Blots were revealed using ECL chemiluminescence reagent detected with Kodak high-speed film (Eastman Kodak, Rochester, NY). The membrane was stripped for 15 minutes (Alpha Diagnostics International, San Antonio, TX) before re-blotting for actin using pan-actin antibodies (1:500, Neomarkers, Fremont, CA) and peroxidase-tagged anti-mouse antibodies (1:5000, Vector Laboratories).

Semi-quantitative densitometry was performed after scanning the film using a Canoscan 4200F plate scanner (Canon, Lake Success, NY) and ArcSoft Photostudio V5.5 software (ArcSoft, Fremont, CA). Images were imported into Image J (National Institutes of Health, Bethseda, MD) and band densities calculated. Band densities were first normalized to actin as a loading control, and then indexed to the standard sample run on each gel.

Deglycosylation Experiments

Deglycosylation of selected LOOP samples was performed with the *N*-Glycanase Enzymatic Deglycosylation Kit (ProZyme, San Leandro, CA) in accordance with the manufacturer's instructions. Briefly, whole-cell lysate, containing 150–200μg of protein, was made up to 20μL volume with reaction buffer. SDS was added (2.5% final volume) and the protein denatured by boiling. NP-40 was added, and either 4μL *N*-Glycanase or water (as a control) was added. The sample was then incubated for 96 hours at 37°C, with regular resuspension of the precipitate. LDS electrophoresis sample buffer (Invitrogen) was added, and the sample reboiled before separating the protein with SDS-PAGE. Protein was transferred to a PVDF membrane, then Western blotting performed for SGLT1 as described above. The experiment was repeated in triplicate with three different LOOP samples.

Statistical Analysis

Transcription data were analysed with post-hoc ANOVA, whilst protein data were analysed with non-parametric tests (Kruskal-Wallis ANOVA). Statistical analysis was performed using Statistica statistical software package (StatSoft, Tulsa, OK). In both cases, diurnal rhythm data were also analysed using the cosinor periodogram analysis program freely available on-line (www.circadian.org), treating the data as a cross-sectional period analysis. For direct comparisons between LOOP and JEJ samples, paired T tests were used. $P<0.05$ was taken as significant. For analysis of molecular weights, observed migration of protein standards was measured and plotted against known weights on a semi-log scale. An exponential line of best fit was then calculated using Microsoft Excel 2000 (Microsoft, Redmond, WA), and the derived equation used to compute the apparent molecular weights of immunoblots.

Results

29 of 38 rats (n=6–8 per time point) survived surgery, remained healthy and gained weight as shown in Figure 1. Mean weight at harvest was 343±2g. The remaining died or were euthanized within the first 48 hours post-operatively, and subsequently excluded from further study. Necropsy showed internal hernias through the either the loop or mesenteric defect with accompanying intestinal obstruction, or anastomostic leak. No other animals were excluded. In all surviving rats, the remnant jejunum exhibited no evidence of edema or distension while the loop was atrophied but was clearly viable and well perfused.

Luminal isolation reduces absorptive surface area

Histology sections confirmed macroscopic impressions that the diameter of LOOP sections was significantly reduced compared to that of JEJ, with major axis diameters 62% greater in JEJ compared to LOOP ($P<0.001$ on paired T tests; see Table 1). However, mucosa within LOOP sections remained viable and healthy (Figure 2), with no significant changes in villus parameters measured, although there was a trend to reduced villus height (24% reduction in height, $P=0.08$) in LOOP sections. Enterocyte diameter was significantly reduced by a similar degree in LOOP sections (25% reduction, $P<0.001$), and it is therefore possible that reduced enterocyte diameter is the underlying etiology of any change in villus parameters.

Sglt1 transcription is independent of local luminal signals

A normal, anticipatory diurnal rhythm was observed in the intact jejunum (JEJ) across the time points studied. Peak *Sglt1* transcription occurred at ZT9, with a 3.2-fold change compared to ZT21 ($P<0.001$ on ANOVA, Figure 3). Wave analysis using cosinor periodicity confirmed diurnal rhythmicity with predicted peak transcription at ZT14, $P<0.001$. Loop samples (LOOP) showed an identical pattern, with a 2.7-fold change compared to ZT21 ($P<0.001$). Again cosinor analysis confirmed a significant diurnal rhythm (acrophase at ZT14, $P<0.001$). *Sglt1* mRNA abundance was similar between LOOP and JEJ at all times ($P=0.08–0.86$) except ZT21, when the LOOP mRNA signal was slightly higher ($P=0.003$).

SGLT1 protein translation is independent of local signals

On immunoblots, the SGLT1 protein had an apparent weight of 69kDa. A representative Western blot is shown in Figure 4. Densitometry of JEJ samples revealed a significant rhythm by ANOVA ($P=0.037$, Kruskal-Wallis ANOVA, Figure 5). The rhythm was similar to that in our previous studies[5,24], but the peak was somewhat earlier than ZT9 with a slightly lower amplitude. Cosinor analysis detected a significant rhythm ($P=0.022$), with an estimated amplitude of 2.4-fold and acrophase at ZT13.

A normal diurnal rhythmicity was observed in loop samples, with peak at ZT15 ($P=0.0116$, Kruskal-Wallis ANOVA, Figure 5). Cosinor analysis confirmed diurnal rhythmicity ($P=0.003$, acrophase at ZT14, 2.1-fold change). Protein expression did not differ between LOOP vs. JEJ samples at any time ($P=0.16–0.99$, paired t test).

Luminal exclusion influences post-translational modifications of SGLT1

Unexpectedly, all LOOP samples contained a more rapidly migrating SGLT1 polypeptide that was absent from almost all JEJ samples (see Figure 4). To determine the difference in molecular weights, a standard curve was generated from the protein markers. By this technique, the apparent molecular weights of the two SGLT1 species were 69kDa and 61kDa, with a difference of 8kDa. Correspondence of this mass to the N-linked oligosaccharide on N-248 suggested that the 69kDa species was the unglycosylated form of SGLT1. To test this possibility, LOOP protein lysates were subjected to enzymatic deglycosylation. Deglycosylation led to disappearance of the 69kDa band, but no change in mobility of the 61kDa band (Figure 6). This result indicates that the 61kDa species is indeed unglycosylated and rather than a truncated SGLT1 protein. This test was repeated a total of three times with different LOOP samples. Densitometry demonstrated that unglycosylated SGLT1 was only a minor component in JEJ samples (2.9±1.5%; $P<0.001$) but had an abundance similar to that of native SGLT1 in LOOP samples (110±12%).

Discussion

The anticipatory diurnal rhythms in SGLT1 expression and function presumably serve to match glucose transport capacity to expected nutrient intake. Potential entraining signals could originate locally (intestinal lumen) and/or systemically (via neural or hormonal pathways). In this study, we tested for the presence of a local signaling mechanism by examining SGLT1 rhythmicity in isolated jejunal loops. Our results demonstrate that both SGLT1 transcription and translation are independent of local luminal nutrients and, therefore, suggest that the entrainment mechanism is predominantly systemic rather than local. We demonstrated very similar levels of SGLT1 expression between isolated loops and jejunum. However, it is important to note that all the Thiry-Vella loops were atrophic, in accordance with multiple previous reports of isolated loops. We did not measure functional glucose transport capacity (due to limited availability of tissue for the required assays, and difficulty mounting the atrophic loops as everted sleeves), and it is important to note that the macroscopic changes in the loops

may have further influences on functional glucose uptake which cannot be accounted for in this study. We did notice a slight non-significant increase in SGLT1 protein expression at ZT9 in JEJ compared to LOOP samples. Importantly, rhythm analysis suggested very similar acrophases, with peak predicted expression at ZT13 and ZT14 respectively. Furthermore, we note a small significant increase in the baseline (ZT21) transcription of *Sglt1*; the significance of this is difficult to interpret as the transcription rate is comparatively low. Furthermore, it may simply reflect differing topographical location of the LOOP compared to the JEJ sections.

The persistence of SGLT1 rhythmicity following isolation of jejunal loops for 10 days, a period longer than necessary to shift the rhythm[19], provides direct evidence for its independence from local luminal nutrients. Our conclusion is supported by several previous studies. Circumvention of the intestinal lumen by parenteral nutrient delivery demonstrated that diurnal rhythmicity of glucose transport and disaccharidase activity[25] could be maintained by discontinuous delivery but was abolished by continuous delivery. In addition to showing independence from luminal nutrients, this result suggested that rhythmicity is not an inherent property of the intestine and that systemic nutrient delivery is sufficient to activate the diurnal entrainment pathway. Further evidence of SGLT1 regulation via systemic signals was derived from studies of the post-prandial increase in canine jejunal absorptive capacity[26,27]. In this model, jejunal feeding led to a rapid upregulation in the water and glucose uptake capacity of the Thiry-Vella loop with properties characteristic of SGLT1[28]. While diurnal changes were not examined, this study does support reliance on systemic signaling for SGLT1 regulation. Of interest, local anesthetic agents suggested that co-ordination of SGLT1 regulation occurred through neural pathways[29]. Similarly, diurnal rhythmicity of sucrase persisted in blind jejunal sacs, a model also designed to test the requirement for luminal signaling[30]. In contrast similar experiments in Burmese pythons (which show rapid upregulation in glucose transport capacity after feeding) showed dissociation between absorptive capacity in the loop and the jejunum, at least in the first few days[31]. However, the much stronger reliance of the python mucosa on luminal nutrients may reflect the dramatic cycles of atrophy and proliferation resulting from its eating rhythms[32].

We have previously demonstrated that the anticipatory rhythm in *Sglt1* transcription is independent of vagal innervation[24]. We now demonstrate that it is regulated at a whole bowel level and is independent of local luminal nutrients or proximal pancreaticobiliary paracrine signals. This suggests that endocrine hormonal control may regulate *Sglt1* transcription, either directly or indirectly through for example peripheral oscillator genes[33–35]. In particular, corticosteroids have been implicated in the co-ordination of peripheral circadian clocks[36], and there is circumstantial evidence linking corticosteroid hormones to the regulation of intestinal hexose transporters[37]. Whilst the enteric nervous system remains a possible co-ordinator of *Sglt1* transcription, the Thiry-Vella loop and hence intrinsic nervous system was isolated from the remainder of the bowel. Thus, if the enteric nervous system is important in the cuing of *Sglt1* transcription, it must be receiving external systemic cues. Nevertheless, extrinsic innervations, such as sympathetic pathways, remained intact and are possible cuing pathways. Furthermore, there remains the possibility that the anticipatory rhythm in the loop was residual from rhythms entrained prior to surgery. However, previous studies with extended fasts in rodents show loss of protein rhythmicity after four days, therefore residual rhythmicity is less likely[19]. This study has further shown that SGLT1 protein rhythmicity is independent of local luminal factors, consistent with the previous demonstration that it is regulated by vagal pathways.

We report in this study the surprising finding of an apparent change in the electromobility of SGLT1. This supports previous findings by Motohashi et al., in experiments using transplanted isolated jejunal loops in rats[38]. This group showed a similar magnitude shift in the apparent molecular weight of SGLT1, as well as reporting a reduction in SGLT1 expression that was at

least partly due to acute graft rejection. They did not, however, further investigate the etiology of the shift in SGLT1 electromobility. This change in apparent molecular weight suggests disruption of the normal post-translational handling of SGLT1, with likely possibilities being either a truncated protein (due to disrupted translation or enhanced proteolysis) or failure of glycosylation. Our deglycosylation experiments suggested that this is a deglycosylated SGLT1 rather than a truncated protein, as deglycosylation increased the mobility of the mature protein with no change in the more mobile band. As glycosylation occurs when the protein trafficks the *trans*-Golgi apparatus, this suggests that luminal isolation may lead to trafficking arrest of SGLT1. The luminal substrate regulating post-translational handling of SGLT1 remains unknown, as does the pathway by which this is mediated. However, we note inhibition of constitutive nitric oxide synthesis within enterocytes has recently been reported to inhibit glycosylation of SGLT1, leading to similar shifts in apparent molecular weight[39]. It is possible therefore that exclusion from enteric passage inhibits constitutive nitric oxide synthase, leading to trafficking arrest of SGLT1.

While we suggest the changes in apparent molecular weight reflect the presence of an unglycosylated SGLT1, it remains unclear whether this represents SGLT1 that has failed to undergo glycosylation (for example, due to trafficking arrest) or has been actively deglycosylated. If the latter, this would suggest a physiological role for the phenomenon by limiting SGLT1 activity.

In summary, we have demonstrated that local luminal nutrients are not required for the maintenance of diurnal rhythms in SGLT1 transcription and translation, although they may exert a direct effect on the post-translational handling of SGLT1.

Acknowledgments

We thank Jan Rounds for invaluable managerial assistance. This study is supported by National Institute of Health 5 R01 DK047326 (SWA), Harvard Clinical Nutrition Center Grant P30-DK040561 (AT), American Diabetes Association 7-05-RA-121 (DBR), Berkeley Fellowship (ATS) and the Nutricia Research Foundation (AB).

References

1. Hediger MA, Coady MJ, Ikeda TS, Wright EM. Expression cloning and cDNA sequencing of the Na +/glucose co-transporter. Nature 1987;330(6146):379–381. [PubMed: 2446136]
2. Hediger MA, Rhoads DB. Molecular physiology of sodium-glucose cotransporters. Physiol Rev 1994;74(4):993–1026. [PubMed: 7938229]
3. Lane JS, Whang EE, Rigberg DA, Hines OJ, Kwan D, Zinner MJ, McFadden DW, Diamond J, Ashley SW. Paracellular glucose transport plays a minor role in the unanesthetized dog. Am J Physiol 1999;276(3 Pt 1):G789–794. [PubMed: 10070058]
4. Pencek RR, Koyama Y, Lacy DB, James FD, Fueger PT, Jabbour K, Williams PE, Wasserman DH. Transporter-mediated absorption is the primary route of entry and is required for passive absorption of intestinal glucose into the blood of conscious dogs. J Nutr 2002;132(7):1929–1934. [PubMed: 12097672]
5. Balakrishnan A, Tavakkolizadeh A, Stearns A, Rounds J, Giuffrida M, Jennifer LI, Rhoads D, Ashley SW. SGLT1-Mediated glucose uptake in jejunum: Diurnal rhythm in intestinal function. Gastroenterology 2007;132(4):A891–A892.
6. Dyer J, Garner A, Wood IS, Sharma AK, Chandranath I, Shirazi-Beechey SP. Changes in the levels of intestinal Na+/glucose co-transporter (SGLT1) in experimental diabetes. Biochem Soc Trans 1997;25(3):479S. [PubMed: 9388700]
7. Burant CF, Flink S, DePaoli AM, Chen J, Lee WS, Hediger MA, Buse JB, Chang EB. Small intestine hexose transport in experimental diabetes. Increased transporter mRNA and protein expression in enterocytes. J Clin Invest 1994;93(2):578–585. [PubMed: 8113395]

8. Fedorak RN, Cheeseman CI, Thomson AB, Porter VM. Altered glucose carrier expression: mechanism of intestinal adaptation during streptozocin-induced diabetes in rats. Am J Physiol 1991;261(4 Pt 1):G585–591. [PubMed: 1928347]
9. Dyer J, Wood IS, Palejwala A, Ellis A, Shirazi-Beechey SP. Expression of monosaccharide transporters in intestine of diabetic humans. Am J Physiol Gastrointest Liver Physiol 2002;282(2):G241–248. [PubMed: 11804845]
10. Osswald C, Baumgarten K, Stumpel F, Gorboulev V, Akimjanova M, Knobeloch KP, Horak I, Kluge R, Joost HG, Koepsell H. Mice without the regulator gene Rsc1A1 exhibit increased Na+-D-glucose cotransport in small intestine and develop obesity. Mol Cell Biol 2005;25(1):78–87. [PubMed: 15601832]
11. Hediger MA, Turk E, Wright EM. Homology of the human intestinal Na+/glucose and Escherichia coli Na+/proline cotransporters. Proc Natl Acad Sci U S A 1989;86(15):5748–5752. [PubMed: 2490366]
12. Hediger MA, Mendlein J, Lee HS, Wright EM. Biosynthesis of the cloned intestinal Na+/glucose cotransporter. Biochim Biophys Acta 1991;1064(2):360–364. [PubMed: 1903656]
13. Hirayama BA, Wright EM. Glycosylation of the rabbit intestinal brush border Na+/glucose cotransporter. Biochim Biophys Acta 1992;1103(1):37–44. [PubMed: 1730019]
14. Hirayama BA, Wong HC, Smith CD, Hagenbuch BA, Hediger MA, Wright EM. Intestinal and renal Na+/glucose cotransporters share common structures. Am J Physiol 1991;261(2 Pt 1):C296–304. [PubMed: 1714681]
15. Turk E, Kerner CJ, Lostao MP, Wright EM. Membrane topology of the human Na+/glucose cotransporter SGLT1. J Biol Chem 1996;271(4):1925–1934. [PubMed: 8567640]
16. Martin MG, Lostao MP, Turk E, Lam J, Kreman M, Wright EM. Compound missense mutations in the sodium/D-glucose cotransporter result in trafficking defects. Gastroenterology 1997;112(4): 1206–1212. [PubMed: 9098004]
17. Rhoads DB, Rosenbaum DH, Unsal H, Isselbacher KJ, Levitsky LL. Circadian periodicity of intestinal Na+/glucose cotransporter 1 mRNA levels is transcriptionally regulated. J Biol Chem 1998;273(16): 9510–9516. [PubMed: 9545279]
18. Tavakkolizadeh A, Berger UV, Shen KR, Levitsky LL, Zinner MJ, Hediger MA, Ashley SW, Whang EE, Rhoads DB. Diurnal rhythmicity in intestinal SGLT-1 function, V(max), and mRNA expression topography. Am J Physiol Gastrointest Liver Physiol 2001;280(2):G209–215. [PubMed: 11208542]
19. Pan X, Terada T, Okuda M, Inui K. The diurnal rhythm of the intestinal transporters SGLT1 and PEPT1 is regulated by the feeding conditions in rats. J Nutr 2004;134(9):2211–2215. [PubMed: 15333706]
20. Stevenson NR, Ferrigni F, Parnicky K, Day S, Fierstein JS. Effect of changes in feeding schedule on the diurnal rhythms and daily activity levels of intestinal brush border enzymes and transport systems. Biochim Biophys Acta 1975;406(1):131–145. [PubMed: 240440]
21. Houghton SG, Iqbal CW, Duenes JA, Fatima J, Kasparek MS, Sarr MG. Coordinated, diurnal hexose transporter expression in rat small bowel: implications for small bowel resection. Surgery 2008;143 (1):79–93. [PubMed: 18154936]
22. Stevenson NR, Fierstein JS. Circadian rhythms of intestinal sucrase and glucose transport: cued by time of feeding. Am J Physiol 1976;230(3):731–735. [PubMed: 1266977]
23. Lanza-Jacoby S, Sitren HS, Stevenson NR, Rosato FE. Changes in circadian rhythmicity of liver and serum parameters in rats fed a total parenteral nutrition solution by continuous and discontinuous intravenous or intragastric infusion. JPEN J Parenter Enteral Nutr 1982;6(6):496–502. [PubMed: 6820074]
24. Stearns AT, Balakrishnan A, Rounds J, Rhoads DB, Ashley SW, Tavakkolizadeh A. Capsaicin-sensitive vagal afferents modulate posttranscriptional regulation of the rat Na+/glucose cotransporter SGLT1. Am J Physiol Gastrointest Liver Physiol 2008;294(4):G1078–1083. [PubMed: 18308853]
25. Stevenson NR, Sitren HS, Furuya S. Circadian rhythmicity in several small intestinal functions is independent of use of the intestine. Am J Physiol 1980;238(3):G203–207. [PubMed: 6102847]
26. Yeo CJ, Bastidas JA, Schmieg RE Jr, Zinner MJ. Meal-stimulated absorption of water and electrolytes in canine jejunum. Am J Physiol 1990;259(3 Pt 1):G402–409. [PubMed: 2399984]

27. Bastidas JA, Zinner MJ, Orandle MS, Yeo CJ. Influence of meal composition on canine jejunal water and electrolyte absorption. Gastroenterology 1992;102(2):486–492. [PubMed: 1732119]
28. Hines OJ, Whang EE, Bilchik AJ, Zinner MJ, Welton ML, Lane J, McFadden DW, Ashley SW. Role of Na+-glucose cotransport in jejunal meal-induced absorption. Dig Dis Sci 2000;45(1):1–6. [PubMed: 10695605]
29. Anthone GJ, Wang BH, Zinner MJ, Orandle MS, Yeo CJ. Meal-induced jejunal absorption requires intact neural pathways. Am J Surg 1992;163(1):150–156. [PubMed: 1310242]
30. Saito M, Sato Y, Suda M. Circadian rhythm and dietary response of disaccharidase activities in isolated rat jejunum. Gastroenterology 1978;75(5):828–831. [PubMed: 359402]
31. Secor SM, Whang EE, Lane JS, Ashley SW, Diamond J. Luminal and systemic signals trigger intestinal adaptation in the juvenile python. Am J Physiol Gastrointest Liver Physiol 2000;279 (6):G1177–1187. [PubMed: 11093940]
32. Secor SM, Diamond J. A vertebrate model of extreme physiological regulation. Nature 1998;395 (6703):659–662. [PubMed: 9790187]
33. Hoogerwerf WA, Hellmich HL, Cornelissen G, Halberg F, Shahinian VB, Bostwick J, Savidge TC, Cassone VM. Clock gene expression in the murine gastrointestinal tract: endogenous rhythmicity and effects of a feeding regimen. Gastroenterology 2007;133(4):1250–1260. [PubMed: 17919497]
34. Sladek M, Rybova M, Jindrakova Z, Zemanova Z, Polidarova L, Mrnka L, O'Neill J, Pacha J, Sumova A. Insight into the circadian clock within rat colonic epithelial cells. Gastroenterology 2007;133(4): 1240–1249. [PubMed: 17675004]
35. Saifur Rohman M, Emoto N, Nonaka H, Okura R, Nishimura M, Yagita K, van der Horst GT, Matsuo M, Okamura H, Yokoyama M. Circadian clock genes directly regulate expression of the Na(+)/H(+) exchanger NHE3 in the kidney. Kidney Int 2005;67(4):1410–1419. [PubMed: 15780093]
36. Balsalobre A, Brown SA, Marcacci L, Tronche F, Kellendonk C, Reichardt HM, Schutz G, Schibler U. Resetting of circadian time in peripheral tissues by glucocorticoid signaling. Science 2000;289 (5488):2344–2347. [PubMed: 11009419]
37. Shepherd EJ, Helliwell PA, Mace OJ, Morgan EL, Patel N, Kellett GL. Stress and glucocorticoid inhibit apical GLUT2-trafficking and intestinal glucose absorption in rat small intestine. J Physiol 2004;560(Pt 1):281–290. [PubMed: 15297580]
38. Motohashi H, Masuda S, Katsura T, Saito H, Sakamoto S, Uemoto S, Tanaka K, Inui KI. Expression of peptide transporter following intestinal transplantation in the rat. J Surg Res 2001;99(2):294–300. [PubMed: 11469900]
39. Arthur S, Saha P, Kekuda R, Coon S, Sundaram U. Constitutive nitric oxide (cNO) inhibits Na-glucose co-transport by altering the glycosylation of the SGLT1 co-transporter in the intestinal epithelial cells. Gastroenterology 2008;134(4):A-83.

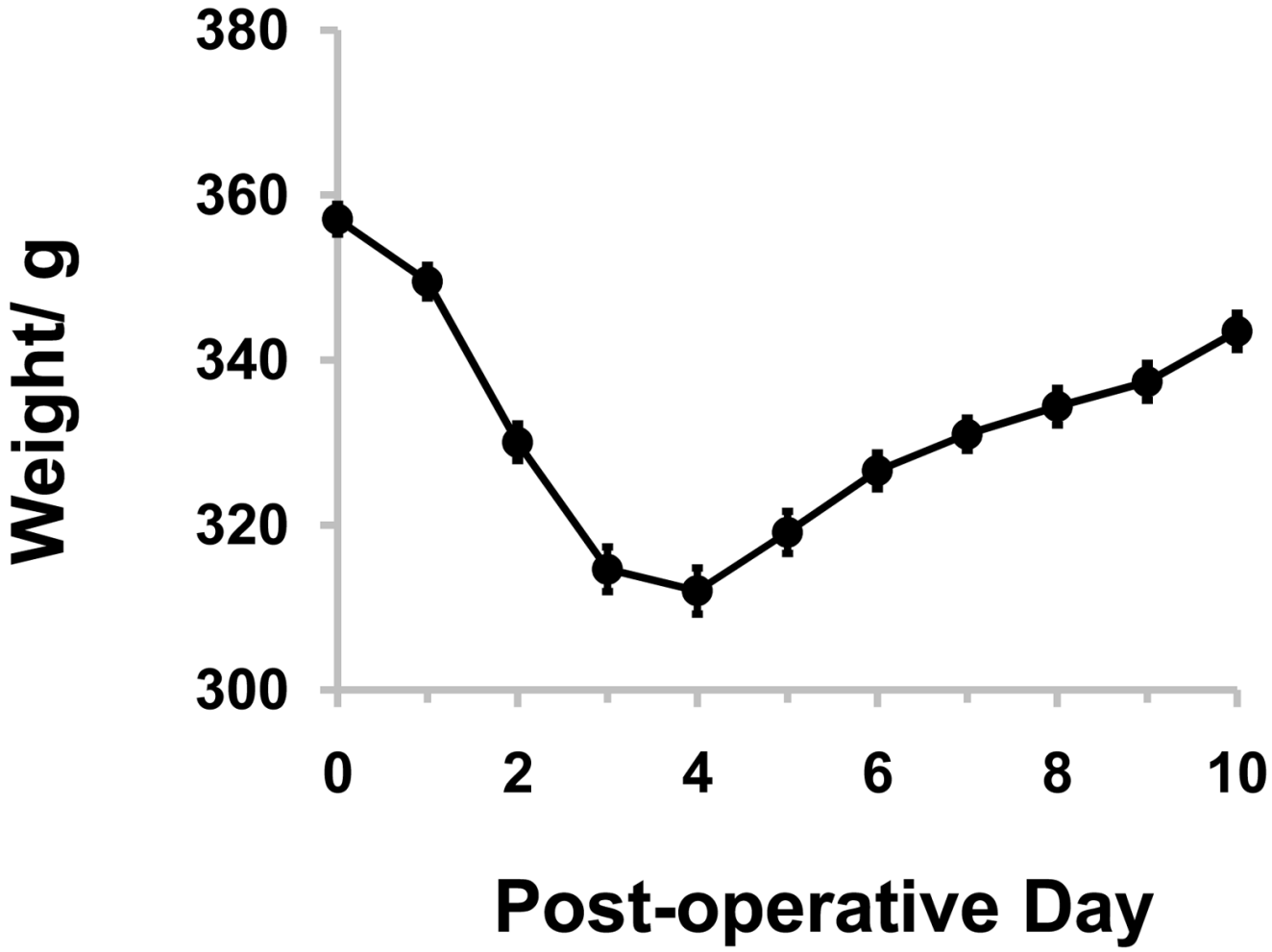

Figure 1.
Mean animal weight after surgery, showing normal weight gain by the end of the experiment. The day of surgery is Day 0. Plots show mean data, while error bars display standard error of the mean; n=29.

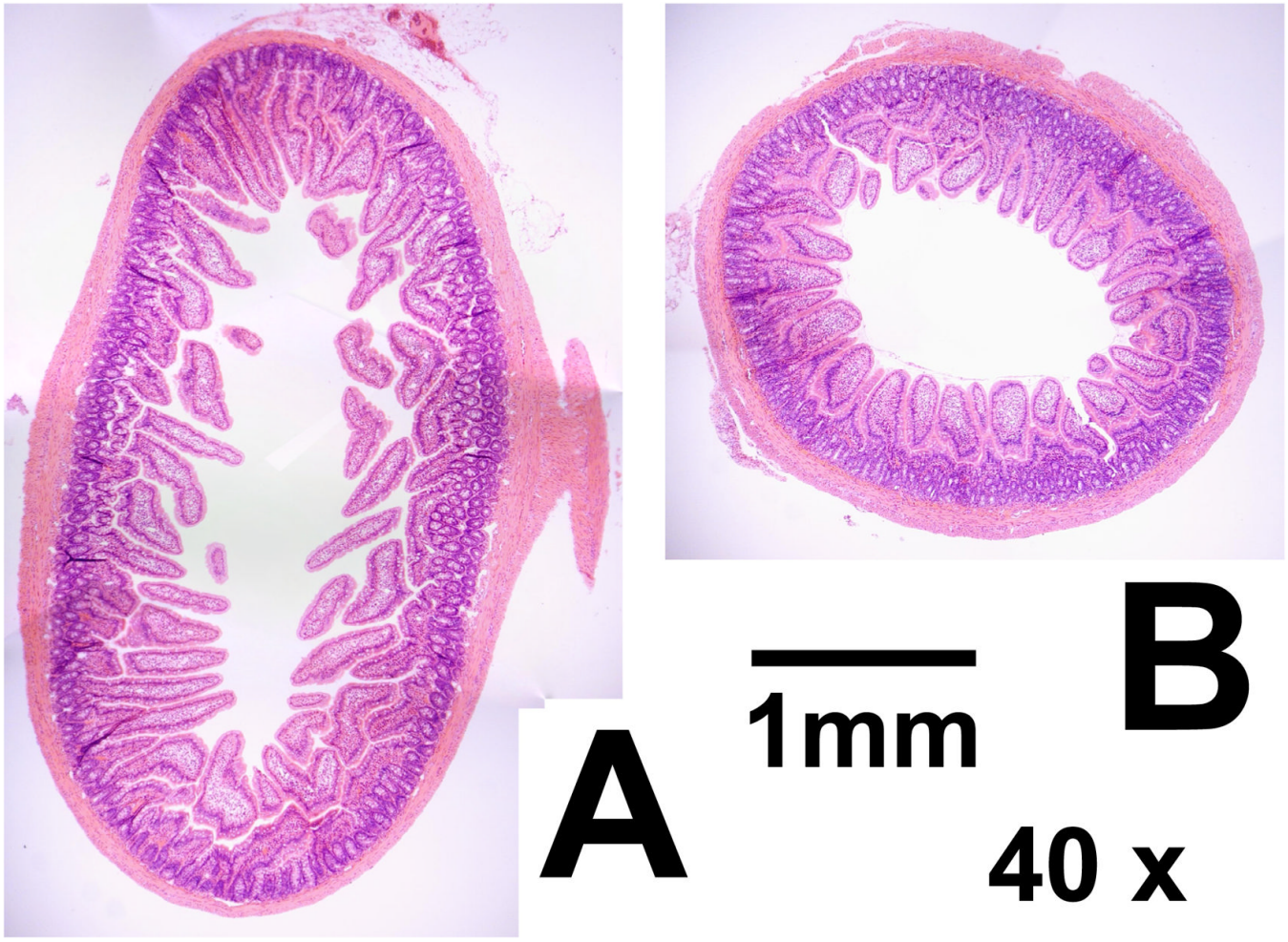

Figure 2.
Representative composite photomicrographs of sections from JEJ (A) and LOOP (B) under 40x magnification. Both sections are from the same animal. The increased diameter in JEJ sections is apparent, as is the tendency for increased villus height. Crypt depth is unchanged between LOOP and JEJ. The scale bar represents 1mm. JEJ; jejunum in enteric continuity. LOOP; isolated jejunal loop.

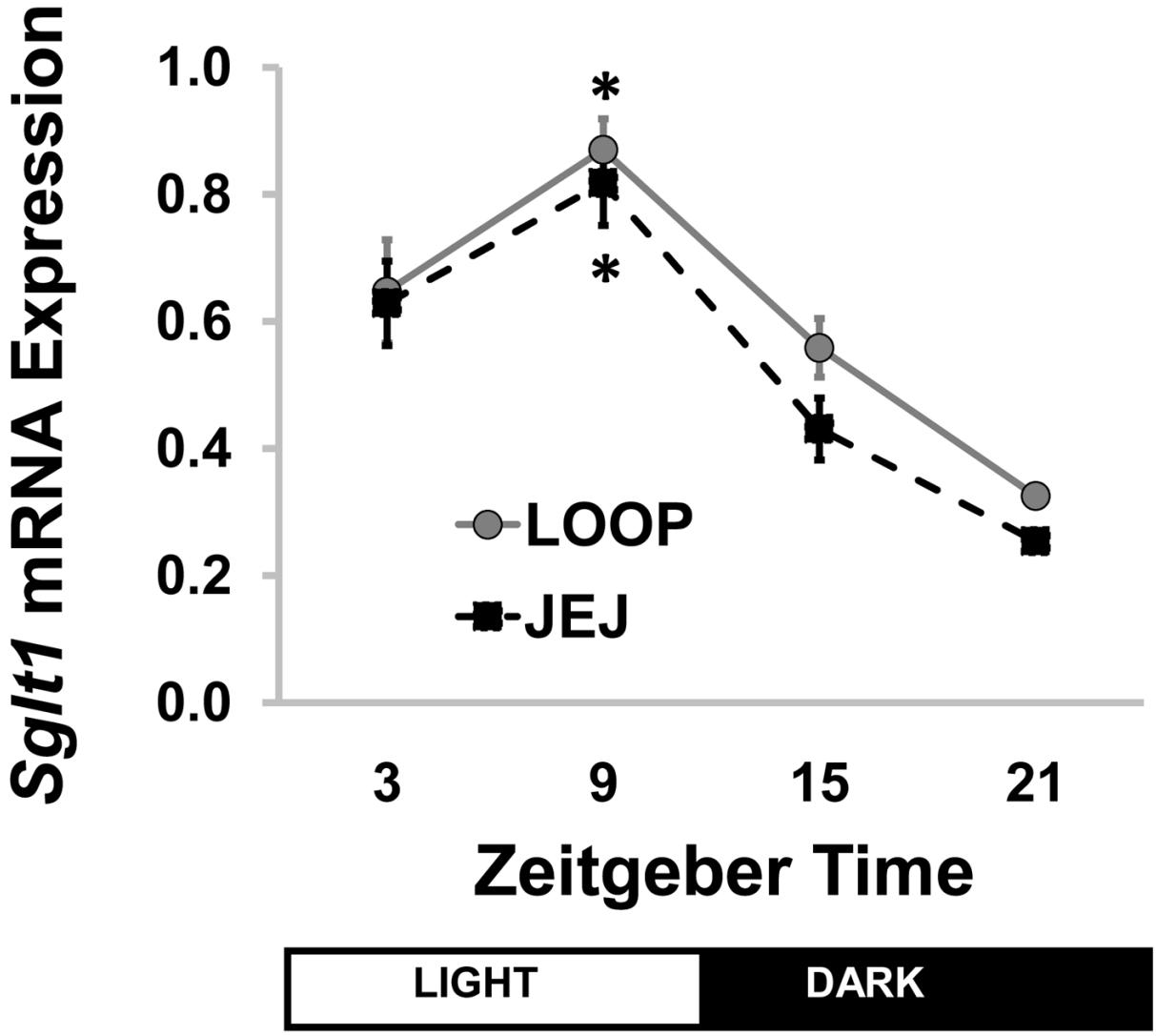

Figure 3.
Sglt1 transcription across diurnal time points in isolated loop (LOOP) and jejunum (JEJ), showing an anticipatory rhythm in both (* $P<0.001$ compared to ZT21). Points show means ± standard error; n=6–8. JEJ: jejunum in enteric continuity; LOOP: isolated jejunal loop; SGLT1: sodium-glucose cotransporter 1; ZT: Zeitgeber time.

Figure 4.
Representative immunoblot for SGLT1, showing a clear diurnal rhythmicity in both intact jejunum (JEJ) and isolated loop (LOOP) mucosa. Of note, an additional band was observed at 61kDa on all loop specimens, but none of the jejunal samples. JEJ: jejunum in enteric continuity; LOOP: isolated jejunal loop; SGLT1: sodium-glucose cotransporter 1.

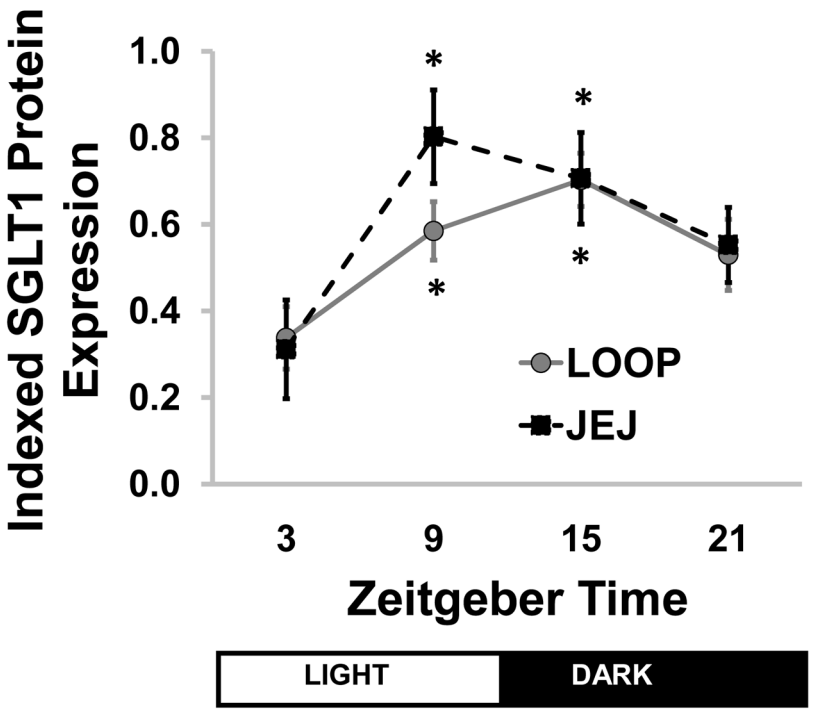

Figure 5.

Semi-quantitative densitometry for SGLT1 protein expression against time. A clear diurnal rhythmicity is seen across the diurnal period in both Thiry-Vella loop (LOOP) and jejunal (JEJ) samples. Protein data has been indexed to a standard sample. * $P<0.05$ compared to ZT3. Points show means ± standard error; n=6–8. SGLT1: sodium-glucose cotransporter 1; ZT: Zeitgeber time.

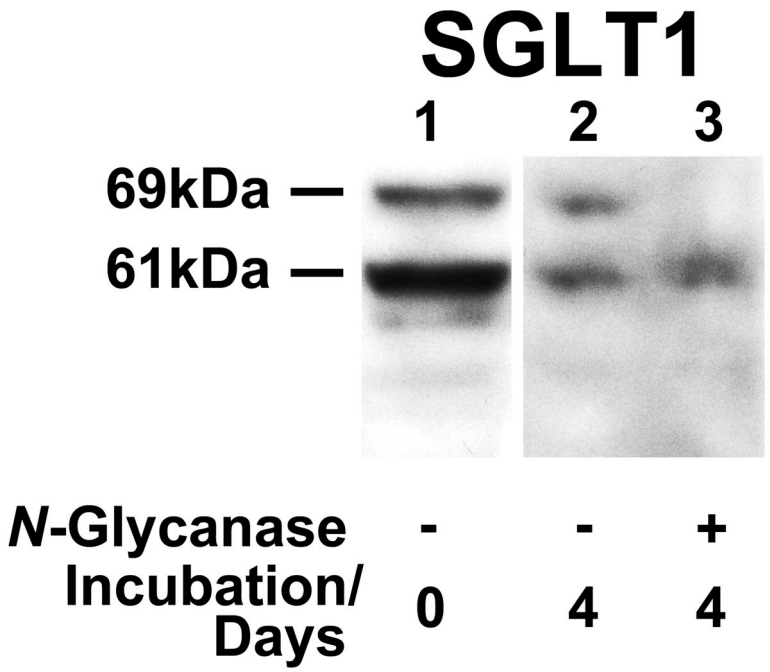

Figure 6.

A representative Western blot from enzymatic deglycosylation experiments, showing 200μg of protein incubated with water (Lane 2, control) or 4μL *N*-glycanase (Lane 3) for four days at 37°C. Lane 1 is an untreated control. The band for SGLT1 holoprotein at 69kDa is lost after deglycosylation, but there is no shift in apparent weight of the 61kDa protein. Experiments were repeated in triplicate using three different LOOP samples. SGLT1: sodium-glucose cotransporter 1.

Table 1

Summary data for morphological analysis of the Thiry-Vella loops, with data taken from samples harvested at ZT15 (10PM, n=7).

Parameter	**JEJ**	**LOOP**	***P* Value**
$Diameter_{max}$	5.0±0.2mm	3.1±0.2mm	<0.0001
$Diameter_{min}$	2.0±0.2mm	1.8±0.1mm	0.39
Villus Height	510±41μm	390±29μm	0.08
Villus Width at Tip	100±6μm	100±7μm	0.97
Villus Width at Base	145±9μm	160±17μm	0.39
Crypt Depth	210±9μm	200±9μm	0.77
Enterocyte Diameter	7.3±0.2μm	5.5±0.1μm	<0.0001

Data presented represents mean ± standard error; *P* values calculated using two tailed paired T tests. JEJ: jejunum in enteric continuity; LOOP: isolated jejunal loop; $Diameter_{max}$: major axis diameter; Diametermin: minor axis diameter, perpendicular to the mid-point of the major axis.